A VARIATIONAL SEGMENTATION FRAMEWORK USING ACTIVE CONTOURS AND THRESHOLDING.

Samuel Dambreville, Marc Niethammer, Anthony Yezzi and Allen Tannenbaum
School of Electrical and Computer Engineering
Georgia Institute of Technology

ABSTRACT
Segmentation involves separating distinct regions in an image. In this note, we present a novel variational approach to perform this task. We propose an energy functional that naturally combines two segmentation techniques usually applied separately: intensity thresholding and geometric active contours. Although our method can deal with more complex image statistics, intensity averages are used to separate regions, in this present work. The proposed approach affords interesting properties that can lead to sensible segmentation results.

KEY WORDS
Image segmentation, curve evolution, PDE, level-set methods, thresholding, parametric estimation.

1 Introduction

Segmentation involves separating an image into distinct regions, a ubiquitous task in computer vision applications. Active contours and image threshholding are among the most important techniques for performing this task.

In the geometric active contour (GAC) framework, a closed curve is represented implicitly as the zero level-set of a higher dimensional function, usually a signed distance function [1]. The curve is evolved to minimize a well-chosen energy functional, typically via gradient descent (see e.g., [1, 2, 3]). The implicit representation allows the curve to naturally undergo topological changes, such as splitting and merging. Different models have been proposed to perform segmentation with GACs: Some frameworks use local image features such as edges [4, 5], whereas other methods use regional image information such a intensity statistics, color or texture [6, 7, 8, 9]. Region based approaches usually offer a higher level of robustness to noise than techniques based on local information. Many of the region-based models have been inspired by the region competition technique proposed in [10]. The book [11] is a nice general reference on the various variational segmentation methods. In region-based frameworks, the intensity statistics of the image are estimated from the segmenting curve using parametric [7, 6] or non-parametric [8] methods. Although nonparametric approaches allow to deal with a wide class of images, parametric methods usually result in simple and efficient segmentation algorithms.

In this note, we propose a novel region-based segmentation technique with GACs. Although the proposed method is general enough to deal with diverse image statistics, we use intensity means only to separate regions, in this work. Hence, our approach is close to the parametric techniques proposed in [7, 6]. However, the way image statistics are used in our framework is different and the resulting flow exhibits distinctive properties. We define a smooth energy functional that allows to employ the result of thresholding the image in order to evolve the contour. Prior reference to this work was made in [12], where the variation of the thresholded image was discarded. We consider the full variation of the proposed energy here and study the resulting flow thoroughly.

The literature about image thresholding is large, and a complete survey is beyond the scope of this paper. The book [13] offers a nice introduction to classical thresholding techniques. Even if a simple thresholding technique is used in this work, the power of the method emanates from the combination with GACs that can naturally split or merge as well as focus on a localized portion of the image.

In what follows, we first present our method and resulting flow. Then, we report experiments that highlight the specificity and power of the technique.

2 Proposed approach: GAC and Thresholding

We consider the problem of segmenting an image $I : \Omega \mapsto \mathcal{Z}$, with $\Omega \subset \mathbf{R}^2$ and $\mathcal{Z}$ the space of possible intensity values (grey-scale). Let $x \in \Omega$ specify the coordinates of the pixels in the image I. Following [7, 6], we assume that I is composed of two (unknown) homogeneous regions, referred to as "Object" and "Background", that have distinct pixel intensity averages μ_{O} and μ_{B} (also unknown). The goal of segmentation is to capture these two regions. To do so, we evolve a closed curve C, represented as the zero level-set of a signed distance function $\phi : \Omega \mapsto \mathbf{R}$, such that $\phi > 0$ inside C and $\phi < 0$ outside C. Our goal is to evolve the contour C, or equivalently ϕ, so that its interior matches the Object, and its exterior matches the Background: the curve C would then match the boundary separating Object and Background.

Let us denote the Heaviside step function by $H : \mathbf{R} \mapsto \{0, 1\}$. A smooth version of H, denoted $H_\epsilon : \mathbf{R} \mapsto$

$[0,1]$, can be computed for a chosen parameter ϵ, as

$$H_\epsilon(\chi) = \begin{cases} = 1 & \text{If } \chi > \epsilon \ ; \\ = 0 & \text{If } \chi < -\epsilon \ ; \\ = \frac{1}{2}\{1 + \frac{\chi}{\epsilon} + \frac{1}{\pi}\sin\left(\frac{\pi\chi}{\epsilon}\right)\} & \text{otherwise} \end{cases} \tag{1}$$

The derivative of H_ϵ will be denoted by δ_ϵ ($\delta_\epsilon(\chi) = 0$ if $|\chi| > \epsilon$; and $\delta_\epsilon(\chi) = \frac{1}{2\epsilon}\{1 + \cos\left(\frac{\pi\chi}{\epsilon}\right)\}$ otherwise). In this note, a region $\mathcal{R} \subset \Omega$ is characterized by a smooth labeling function $\mathrm{R}_\mathcal{R} : \Omega \mapsto [0,1]$ such as $\mathrm{R}_\mathcal{R}(x) \geq \frac{1}{2}$ if $x \in \mathcal{R}$ & $\mathrm{R}_\mathcal{R}(x) < \frac{1}{2}$ if $x \in \Omega \backslash \mathcal{R}$. Thus, the segmentation defined by the interior of C is characterized by the labeling function $H_{\epsilon_1}\Phi$. [1]

The intensity averages of the pixels located inside and outside the curve C, denoted by μ_{in} and μ_{out} respectively, can be computed at each iteration of the evolution as $\mu_{\text{in}}(\phi) = \frac{\int_\Omega I(x)H\phi(x)\,dx}{A_{\text{in}}}$ and $\mu_{\text{out}}(\phi) = \frac{\int_\Omega I(x)(1-H\phi(x))\,dx}{A_{\text{out}}}$, where $A_{\text{in}}(\phi) = \int_\Omega H\phi(x)dx$ and $A_{\text{out}}(\phi) = \int_\Omega \big(1 - H\phi(x)\big)dx$ denote the areas inside and outside the curve, respectively. Provided a meaningful initialization of the curve, these statistics bear valuable information about the statistics of the Object and the Background. Intuitively, the intensity averages μ_{in} and μ_{out} are the best estimates of the unknown intensity averages μ_{O} and μ_{B}, respectively. We propose to use μ_{in} and μ_{out} to threshold the image. Let us denote the corresponding labeling function by $G : \Omega \mapsto [0,1]$. The function G is defined so that pixels x that are more likely to belong to the Object are attributed a value $G(x) \geq \frac{1}{2}$, whereas pixels more likely to belong to the Background are attributed a value $G(x) < \frac{1}{2}$. By defining the threshold $\tau(\phi) = \frac{\mu_{\text{in}}+\mu_{\text{out}}}{2}$, a possible candidate for G, for a chosen smoothness parameter ϵ_2, is thus[2] :

$$G(\phi, x) = \begin{cases} H_{\epsilon_2}\big(I(x) - \tau(\phi)\big) & \text{If } \mu_{\text{in}} \geq \mu_{\text{out}} \ ; \\ H_{\epsilon_2}\big(\tau(\phi) - I(x)\big) & \text{If } \mu_{\text{in}} < \mu_{\text{out}} \end{cases} \tag{2}$$

The functional G, which depends on ϕ, is computed at each step of the contour evolution.

To perform segmentation, we propose to minimize

$$\begin{aligned} E_{\text{image}}(\phi, I) &= \|H\phi - G(\phi)\|^2 \\ &= \int_\Omega \{H\phi(x) - G(\phi, x)\}^2 dx \end{aligned} \tag{3}$$

This energy is the L_2 distance between the (*current*) segmentation $H\phi$ obtained from the curve C and the (*implied*) segmentation G obtained from thresholding I. Minimizing this energy makes sense for the purpose of segmentation since it is minimum, i.e. $E_{\text{image}} = 0$, if and only if the curve splits I into two regions which pixel intensities are either above or strictly below $\tau_\infty = \frac{\mu_{\text{O}}+\mu_{\text{B}}}{2}$, respectively. The minimization is performed by evolving C according to the flow:

$$\frac{d\phi}{dt} = -\nabla_\phi E_{\text{image}} \tag{4}$$

The gradient $\nabla_\phi E_{\text{image}}$ can be computed using calculus of variations (both $H\phi$ and G depend on ϕ):

$$\nabla_\phi E_{\text{image}} = 2 \times \delta\phi \times \big(H\phi - G\big) + 2\beta \times \nabla_\phi \tau, \tag{5}$$

where the expressions of $\beta \in \mathbf{R}$ and $\nabla_\phi \tau : \Omega \mapsto \mathbf{R}$ are

$$\begin{aligned} \beta &= s_{\mu_{\text{in}}-\mu_{\text{out}}} \int_\Omega \delta_{\epsilon_2}\big(I(x) - \tau\big)[H\phi(x) - G(x)]dx \\ \nabla_\phi \tau &= \delta\phi \times \frac{1}{2}\big(\frac{\mu_{\text{out}} - I}{A_{\text{out}}} + \frac{I - \mu_{\text{in}}}{A_{\text{in}}}\big) \end{aligned} \tag{6}$$

In equation (6), $s_{\mu_{\text{in}}-\mu_{\text{out}}} = 1$, if $\mu_{\text{in}} \geq \mu_{\text{out}}$; and $s_{\mu_{\text{in}}-\mu_{\text{out}}} = -1$, if $\mu_{\text{in}} < \mu_{\text{out}}$. The gradient $\nabla_\phi E_{\text{image}}$ is the sum of two terms. In the gradient descent process of equation (4), the first term, namely $2 \times \delta\phi \times \big(H\phi - G\big)$, points towards G. This term is comparable to the term $(I - \mu_{\text{out}})^2 - (I - \mu_{\text{in}})^2$ in the gradient obtained by the authors in [7]. Image pixels (in the vicinity of C) which intensities are closer to μ_{in} are included in C, whereas pixels closer to μ_{out} are excluded. An important difference is that the speed is dependent on the intensities values in the flow described in [7]. The second term in $\nabla_\phi E_{\text{image}}$, namely $2\beta \times \delta\phi \times \nabla_\phi \tau$, considers the variation of the mean intensities μ_{in} and μ_{out}, when the curve C evolves. Such a term is not present nor possible in the flow presented in [7]. Depending on the sign of β, this term points in the direction of the fastest increase or decrease of the threshold τ, *resulting in changing* G. The coefficient β is essentially a counting function focusing on the "ambiguous pixels", i.e. pixels which intensities are close to the threshold τ (C.f. the term $\delta(I - \tau)$ in the expression of β) and for which classification is the most uncertain. The sign and magnitude of β are conditioned upon the number of ambiguous pixels that belong to one of the segmentation terms ($H\phi$ or G) but not the other. The systematic treatment of ambiguous pixels afforded by this second term is an important feature of this work, and will be further examined in the experimental part below.

3 Experimental Results

We now present experimental results, using the heuristic $\epsilon_2 = 5 \times \epsilon_1$ for greyscale images $I : \Omega \mapsto \{0..255\}$.

In Figure 1, a synthetic image is segmented to illustrate the particular behavior of our flow. The image is composed of 4 phases: light grey and white ("question mark"), dark grey and back. Figure 1(a), (b), (c), (d), present the evolution of the segmenting curve (top row) and the corresponding thresholded image G (bottom row), when minimizing E_{image}. Figure 1(f)-*top* presents the results obtained when C is evolved using the gradient in [7], with no

[1] For a chosen (small) ϵ_1. In the remainder, we will often omit ϵ_1 in the expressions of $H_{\epsilon_1}\phi$, and $\delta_{\epsilon_1}\phi$, and denote $H\phi$ and $\delta\phi$ to simplify notation.

[2] In the limit case when $\epsilon_2 \to 0$, G is the result of *hard thresholding* the image I, using the threshold τ.

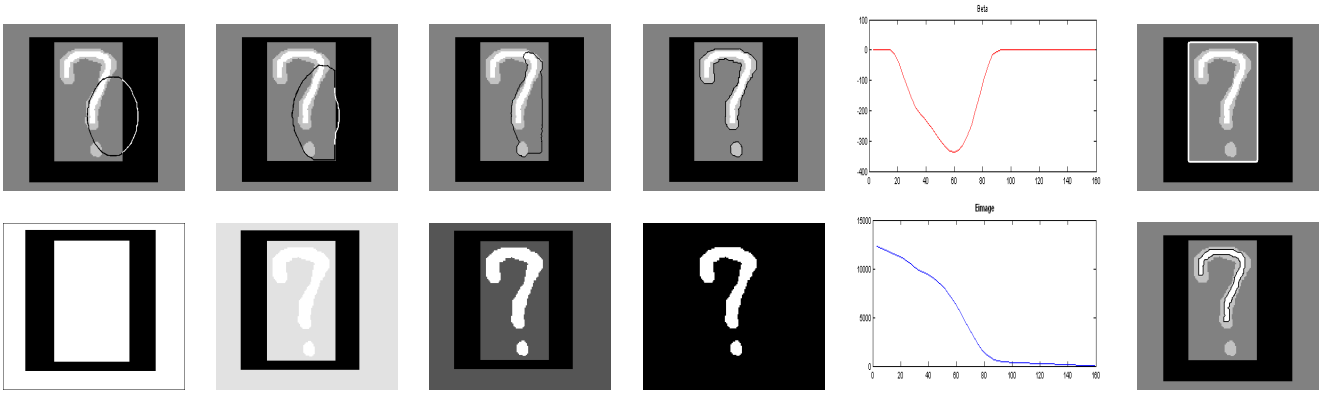

(a) (b) (c) (d) (e) (f)

Figure 1. Toy Example. (a), (b), (c), (d): 4 successive evolution steps minimizing E_{image}; *Top*: Image+Curve (black or white); *Bottom*: Corresponding thresholded Image G. (e)-*Top*: Evolution of β; (e)-*Bottom*: Evolution of E_{image}. (f)-*Top*: White curve, final result with [7]; (f)-*Bottom*: Black curve, final result with [6].

curvature term[3] (see e.g., [3]). Figure 1(f)-*bottom* presents the results obtained when C is evolved using the gradient in [6]. Three different results are obtained using the 3 different techniques: The region inside the curve is "darker" when [7] is used, "lighter" when [6] is used, and a "middle ground" is reached with our technique. When only the first term of ∇E_{image} is used, a similar result as [7] is obtained (Figure 1(f)-*top*), this highlights the influence of the second term of our gradient that we proceed to explain: From the initialization on, we have $\mu_{\text{in}} > \mu_{\text{out}}$, besides there are overall more ambiguous pixels (light grey) in G than inside C. The sign of β is thus negative, as can be checked from the plot of β in Figure 1(e). Following Equation (4), the curve evolves in the direction of $\nabla_\phi \tau$, thus *increasing* the threshold τ. This results notably in eliminating darker image pixels from the segmentation G and from inside the curve. Hence, the second term of ∇E_{image} appears to make meaningful decisions of the type: if more ambiguous pixels are inside C (resp. outside) then take more ambiguous pixels inside C (resp. outside).

Figure 2 presents segmentation results on two synthetic images. In Figure 2(a), (b), (c) an image composed of the word "YELLOW" in dark letters on a linearly shadowed (lighter) background is segmented. Figure 2(b) presents the segmentation result obtained using our technique. Figure 2(c) presents the segmentation result obtained using [7], with no curvature term. Our approach removes pixels from the background and ends up segmenting the word "YELLOW"; a similar result is obtained with the flow of [6]. In Figure 2(d) and (e), we show that objects with smooth contours, which are difficult to segment using edge-based approaches (e.g. [4, 5]), can be segmented with our technique. This type of objects can also be segmented by the method proposed by [7]. However, the contour collapses to a point if the flow in [6] is used.

Figure 3 presents segmentation results of a real image representing two people in winter (Swedish Couple). In Figure 3(c), the flow proposed in [7] was used: The final contour encompasses noisy pixels of the background and lighter shadows. In Figure 3(d), the flow proposed in [6] was used: The final contour encompasses the darkest pixels in the image only. In Figure 3(b), E_{image} was minimized and a "middle ground" is reached, nicely segmenting the two persons.

In Figure 4, MRI-images of the brain are segmented. The corpus callosum (center) is difficult to segment since boundaries are poorly defined, a typical issue in medical images. In Figure 4(c), the method proposed in [7] was used. Despite a large value of the curvature term (maximum possible to allow the initial contour to merge), the curve leaks in the upper part of the brain due to poor contrast with other neighboring structures. In Figure 4(b), our method was used *with no curvature term*. An acceptable segmentation of the corpus callosum, capturing finer details of the structure is obtained.

In Figure 5, an MRI-image of the heart is segmented. An acceptable segmentation of the left ventricle is obtained with our method (*First row, right* in the Figure). A comparable segmentation of this image was obtained in [14], where global constraints were imposed on the flow presented in [6]. The *Second row* of Figure 5, presents the results obtained using the methods proposed in [7] and [6] for comparison. Again, a "middle ground" between [7] and [6] is reached with our method.

4 Conclusions and Future Research

In this work, we presented a variational approach combining two segmentation techniques: active contours and (smooth) thresholding. In the proposed framework, image statistics (intensity averages) are exploited by defining an energy functional that compares the segmentation obtained from the evolving curve with the segmentation obtained

[3] To compare the way image statistics are used across methods.

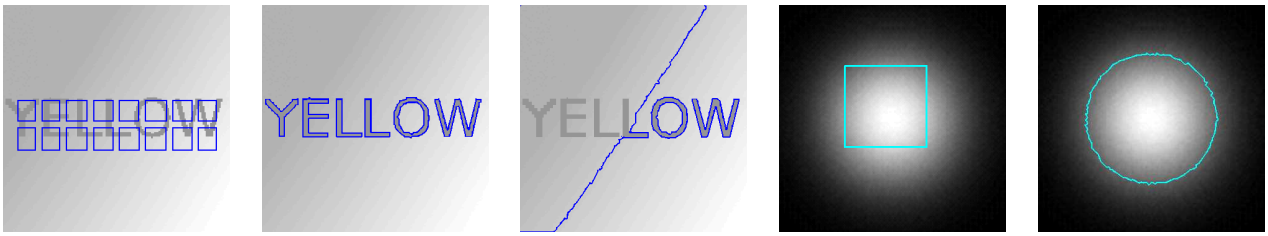

(a) (b) (c) (d) (e)

Figure 2. Synthetic images: Word with linear background & Object with smooth boundary. (a): Initialization; (b): Segmentation result with the proposed method or [6]; (c): Typical result with [7]-no curvature. (d): Initialization; (e): Result using the proposed method.

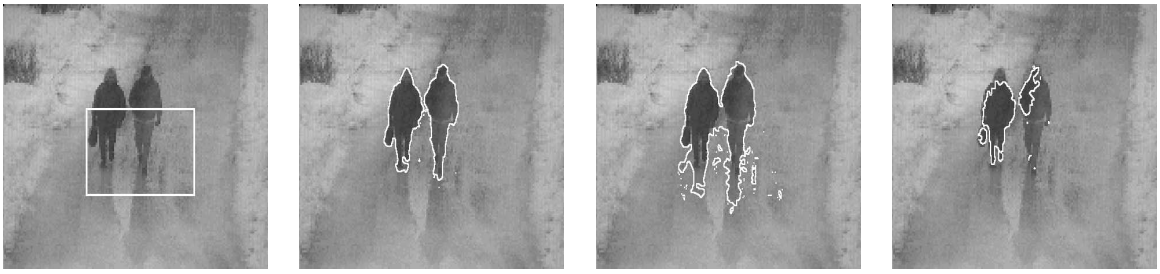

(a) (b) (c) (d)

Figure 3. Segmentation of a real image (Swedish couple). (a): Initialization; (b) Segmentation result with the proposed method; (c) Typical result with [7]; (d) Typical result with [6]. No regularizing term used. The proposed method achieves a "middle ground" between [7] and [6].

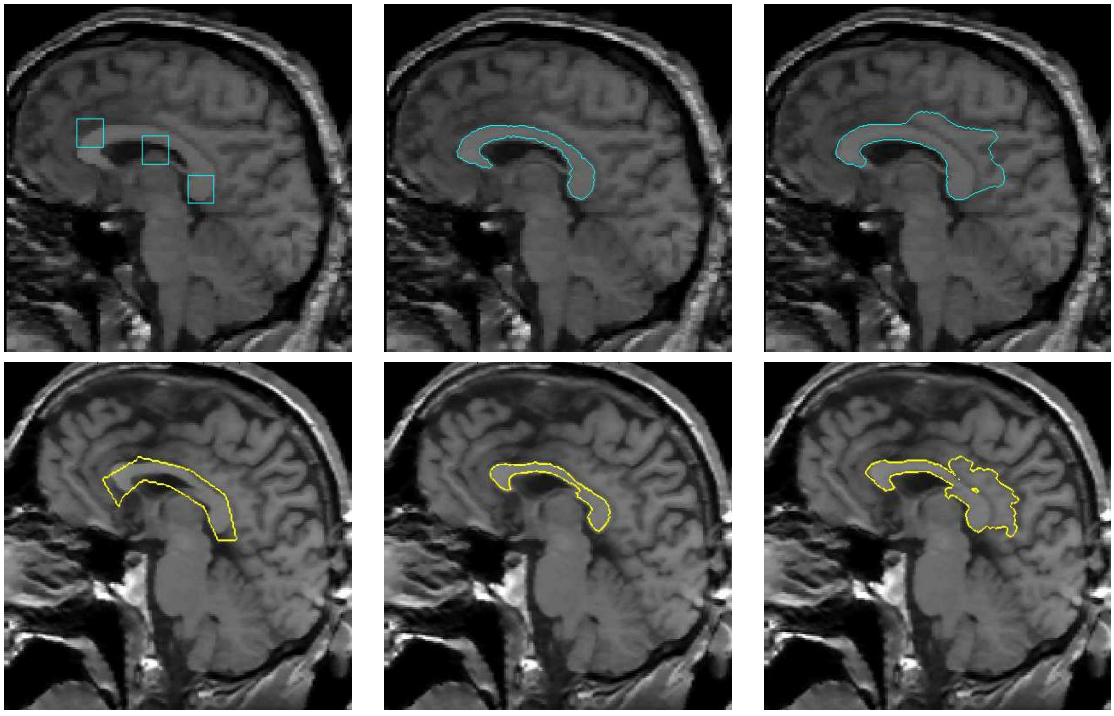

Figure 4. Segmentation results the corpus callosum for two MRI images of the brain. *Left*: Initialization, *Middle*: Segmentation result with the proposed method - no curvature; *Right*: Typical result with [7] - even using a large curvature term.

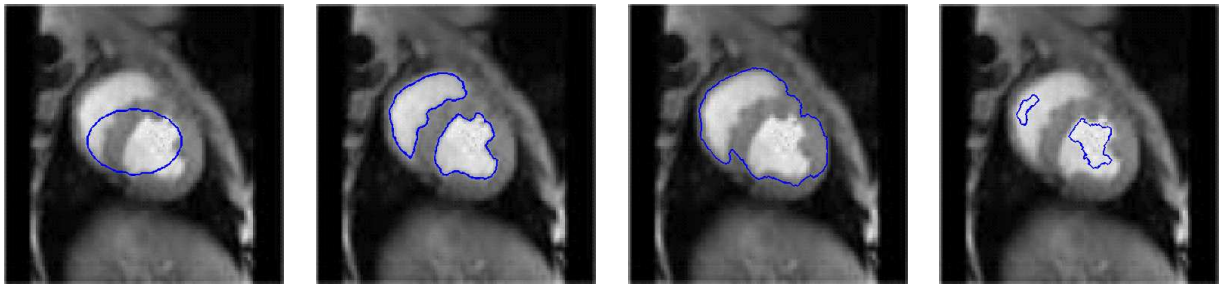

(a) (b) (c) (d)

Figure 5. Segmentations of an MRI image of the heart (Left ventricle). (a): Image and initial contour; (b): Segmentation result, using the proposed framework. (c): Segmentation result with [7] (d): Segmentation result with [6]

from thresholding the image. The resulting flow affords some useful properties allowing the segmenting curve to reach local energy minima that coincide with meaningful segmentations. In our future work, we plan to expand the proposed approach to deal with more complex distributions of pixel intensities.

References

[1] J. A. Sethian, *Level Set Methods and Fast Marching Methods*, 1999.

[2] N Paragios, Y. Chen, and O Faugeras, *Handbook of Mathematical Models in Computer Vision*, Springer, 2005.

[3] S. Osher and R. Fedkiw, *Level Set Methods and Dynamic Implicit Surfaces*, Springer Verlag, 2003.

[4] V.Caselles, R. Kimmel, and G. Sapiro, "Geodesic active contours," in *IJCV*, 1997, vol. 22, pp. 61–79.

[5] S. Kichenassamy, S. Kumar, P. Olver, A. Tannenbaum, and A. Yezzi, "Conformal curvature flow: From phase transitions to active vision," in *Archives for Rational Mechanics and Analysis*, 1996, vol. 134, pp. 275–301.

[6] A. Yezzi, A. Tsai, and A. Willsky, "A statistical approach to snakes for bimodal and trimodal imagery," in *Proc. ICCV*, 1999, vol. 2, pp. 898–903.

[7] T. Chan and L. Vese, "Active contours without edges," *IEEE Trans. on Image Processing*, vol. 10, no. 2, pp. 266–277, 2001.

[8] J. Kim, J. Fisher, A. Yezzi, M. Cetin, and A. Willsky, "Nonparametric methods for image segmentation using information theory and curve evolution," in *Proc. ICIP*, 2002, vol. 3, pp. 797–800.

[9] M. Rousson and R. Deriche, "A variational framework for active and adaptative segmentation of vector valued images," in *Proc. of the Workshop on Motion and Video Computing*, 2002, p. 56.

[10] Song Chun Zhu and Alan L. Yuille, "Region competition: Unifying snakes, region growing, and Bayes/MDL for multiband image segmentation," 1996, vol. 18, pp. 884–900.

[11] J-M Morel and S. Solimini, *Variational Methods for Image Segmentation*, Birkhauser, 1994.

[12] S. Dambreville, Y. Rathi, and A. Tannenbaum., "Shape-based approach to robust image segmentation using kernel pca," in *In IEEE Conference on Computer Vision and Pattern Recognition*, 2006, pp. 977–984.

[13] Rafael C. Gonzalez and Richard E. Woods, *Digital Image Processing*, Addison-Wesley Longman., 2001.

[14] A. Yezzi, A. Tsai, and A. Willsky, "Medical image segmentation via coupled curve evolution equations with global constraints," in *Proc. Workshop on Mathematical Methods in Biomedical Image Analysis*, 2000, pp. 12–19.